

# Characterization of neutrino signals with radiopulses in dense media through the LPM effect

J. Alvarez-Muñiz, R.A. Vázquez, and E. Zas

*Departamento de Física de Partículas, Universidade de Santiago E-15706 Santiago de Compostela, Spain*

We discuss the possibilities of detecting radio pulses from high energy showers in ice, such as those produced by PeV and EeV neutrino interactions. It is shown that the rich radiation pattern structure in the 100 MHz to few GHz allows the separation of electromagnetic showers induced by photons or electrons above 100 PeV from those induced by hadrons. This opens up the possibility of measuring the energy fraction transmitted to the electron in a charged current electron neutrino interaction with adequate sampling of the angular distribution of the signal. The radio technique has the potential to complement conventional high energy neutrino detectors with flavor information.

**PACS number(s):** 96.40.Pq; 96.40.Tv; 95.85.Bh; 13.15.+g

**Keywords:** Cherenkov radiation, LPM effect, Electromagnetic and hadronic showers, Neutrino detection.

High energy neutrino detection is one of the experimental challenges for the next decade with efforts under way to construct large Cherenkov detectors arrays under water or ice [1]. The size of these detectors must be in the scale of 1 km<sup>3</sup> water equivalent to test the neutrino flux predictions above the TeV that arise in a number of models attempting to explain the origin of highest energy observed cosmic rays and gamma rays [2]. EeV fluxes are difficult to avoid both in the production of the highest energy cosmic rays and in the propagation through the cosmic microwave background. Moreover there are allowed regions in parameter space for neutrino oscillations [3] which may be best probed with high energy neutrinos from cosmological or galactic distances [4]. It is thus desirable to explore possibilities for alternative neutrino detection such as horizontal air showers [5] or radio pulses from high energy showers [6,7]. These techniques may be advantageous at sufficiently high energies [8] and can provide in any case complementary information relevant for flavor identification.

The detection of coherent radio waves from high energy showers has been known since the 60's as an interesting alternative for detecting ultra high energy showers [6]. These showers develop large excess negative charge because the vast majority of the shower particles are in the low energy regime dominated by electromagnetic interactions with the electrons in the target (Compton, Bhabha, Möller scattering and electron positron annihilation). The excess charge becomes about 20% of the total number of electrons and positrons (shower size), which is proportional to shower energy. This excess charge ra-

diates coherently. As long as the wavelength is larger than the shower dimensions, the electric field amplitude  $E = |\vec{E}|$  scales with shower energy. The technique has been proposed for detecting neutrino interactions in ice or sand [7]. It has potential advantages such as the relatively low cost of the detectors (antennae), the large attenuation length for radio waves and most importantly the fact that information on the excess charge distribution can, in principle, be reconstructed from the radiation pattern because the radiation is coherent.

When a particle of charge  $z$  travels through a medium of refractive index  $n$  with velocity  $\vec{v} = \beta c > c/n$  Cherenkov light is emitted at the Cherenkov angle  $\theta_C$ , verifying  $\cos \theta_C = (\beta n)^{-1}$ , with a power spectrum given by the well known Frank-Tamm result [9] :

$$\frac{d^2W}{d\nu dl} = \left[ \frac{4\pi^2 \hbar}{c} \alpha \right] z^2 \nu \left[ 1 - \frac{1}{\beta^2 n^2} \right], \quad (1)$$

with  $dl = c\beta dt$ , the particle track, and  $\alpha$  the fine structure constant. This is the standard approximation used for most Cherenkov applications for wavelengths orders of magnitude smaller than the tracks.

The frequency band over which Cherenkov radiation is emitted can extend well beyond the familiar optical band if the medium is transparent. As the radiation wavelength becomes comparable to the particle tracks the emission from all particles is coherent and the excess charge distribution in the shower generates a complex radiation pattern. It is most convenient to work directly with the Fourier transform of the radiated electric field,  $\vec{E}$ , which can be directly obtained from Maxwell's equations in a dielectric medium [11–13]. In the Fraunhofer limit (observation distance  $R$  much greater than the tracklength) the contribution of an infinitesimal particle track  $\vec{\delta l} = \vec{v}\delta t$  is given by:

$$R\vec{E}(\omega, \vec{x}) = \frac{e\mu_r i\omega}{2\pi\epsilon_0 c^2} \vec{\delta l}_\perp e^{i(\omega - \vec{k}\vec{v}_\perp)t_1} e^{ikR}, \quad (2)$$

where  $\vec{k}$ ,  $\vec{k} \parallel \vec{R}$ , is the wave vector in the direction of observation ( $\vec{R}$ ) and  $\vec{l}_\perp$  is the tracklength projected onto a plane perpendicular to the observing direction.

This simple expression displays in a transparent form three most important characteristics of such signals: The proportionality between the electric field amplitude and the tracklength, the fact that in the Cherenkov direction ( $\omega - \vec{k} \cdot \vec{v} = 0$ ) there is no phase factor associated to the position along the track direction and the fact that radiation is polarized in the direction of  $\vec{l}_\perp$ , that is in the

apparent direction of the track as seen from an observer located at  $\vec{x}$ .

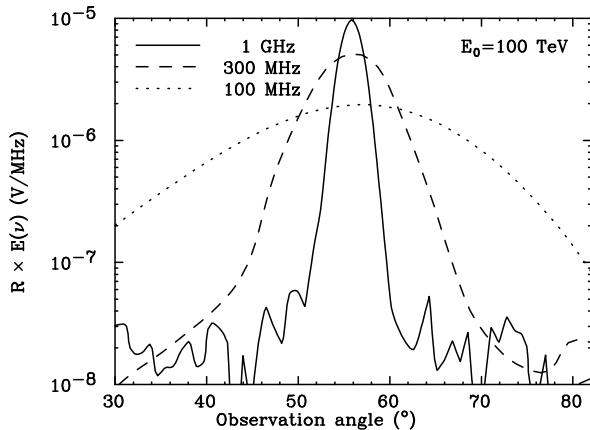


FIG. 1. Electric field angular distribution.

Recent numerical simulations of radio pulses from both electromagnetic and hadronic showers [14,16,17] are based on this expression. For energies below 10 PeV full simulations are possible [14]. The characteristic angular distributions and frequency spectra are shown in Figs. 1,2. We can understand most of the pulse characteristics by studying the particle distributions in a shower as the excess charge follows the electron distribution closely.

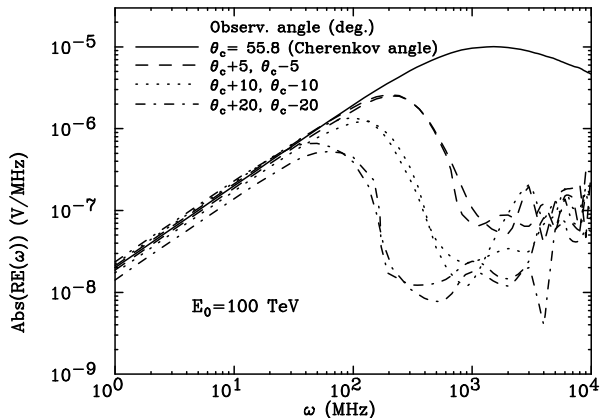


FIG. 2. Electric field frequency spectrum.

To a good approximation the pulse is the Fourier transform of the spatial distribution of the excess charge. For many purposes it is sufficient to study the Fourier transform of the one dimensional distribution (in shower axis  $z$ ) as has been extensively checked [18]:

$$R|\vec{E}(\omega, \vec{x})| \simeq \frac{e\mu_r i\omega}{2\pi\epsilon_0 c^2} e^{ikR} \sin\theta \int dz Q(z)e^{ipz} \quad (3)$$

We here introduce the parameter  $p(\theta, \omega) = \omega/c(1 - n \cos\theta)$  to transparently relate the radio emission spectrum to the Fourier transform of the (excess) charge distribution  $Q(z)$ . This approximation together with hybrid techniques combining simulation and parameterization of shower development have allowed the characterization of pulses from showers of energy up to 100 EeV [16,17].

The angular distribution of the pulse has a main "diffraction" peak corresponding to  $p = 0$ , the Cherenkov direction, see Fig. 1. For  $|p| l_{sh} \ll 1$ , where  $l_{sh}$  is a length scale parameter for the shower [16], the electric field spectrum accurately scales with electron track-length, see Fig. 2. In electromagnetic showers the track-length is proportional to the energy [16] and for hadronic showers it scales with a slowly varying fraction of the energy (80 – 92 % for shower energies between 100 TeV and 100 EeV) [17].

The scaling with electromagnetic energy is broken by interference from different parts of the shower when  $|p| l_{sh} \sim 1$ . As a result the frequency spectrum stops rising linearly with frequency and has a maximum  $\omega_M(\theta)$  which depends strongly on  $\theta$  as seen in Fig. 2. Expanding the condition for  $p(\theta)$  about  $\theta_C$  it simply becomes  $n \sin\theta_C l_{sh} \Delta\theta \omega_M/c \sim 1$  which clearly displays how  $\Delta\theta$  is inversely proportional to  $\omega_M$  as shown in the figure. This allows independent establishment of the angle between the observation and Cherenkov directions which is not sufficient to establish the shower direction but it can be combined with other measurements to provide useful information. This relation however breaks down when approaching the Cherenkov direction because the lateral distribution plays the destructive role although there is no interference from different shower depths (Eq. 2).

The "central peak" at 1 GHz concentrates most of the power. For given frequency the angular spread of the pulse is also inversely proportional to  $l_{sh}$ . This effect hardly shows in showers below 10 PeV with a longitudinal scale that only depends logarithmically on energy [19]. The difference between the longitudinal development of the excess charge for electromagnetic and hadronic showers is not enough to show up in the radiopulse structure (both are governed by the radiation length of the material). Nevertheless the angular width of the pulse reduces significantly for the characteristically elongated electromagnetic showers above 100 PeV because of the LPM effect [20]. This narrowing of the angular distribution allows the identification of elongated showers.

The LPM effect manifests as a dramatic reduction of the pair production and bremsstrahlung cross sections at large energies due to large scale correlations in the atomic electric fields [21,22]. It only affects the development of showers initiated by photons, electrons or positrons above a given energy, about 20 PeV in ice [20]. Showers initi-

ated by EeV hadrons have high multiplicities (50-100) in their first interaction, and the pions produced typically have energies 1 – 2% that of the initial hadron. Moreover  $\pi^0$ 's above 6.7 PeV are more likely to interact in ice than to decay and only about 2% of the hadron showers above 10 EeV have one photon with more than 10% of the hadron energy. Furthermore in a 100 EeV neutrino interaction for example the fraction of energy transferred to the hadron debris (25% in average) fragments into about 17 hadrons (mostly pions) which have about 5% of the transferred energy (except for the leading baryon which would carry a fraction  $1 - K$  where  $K$  is the inelasticity). As a result the photons that are responsible for the electromagnetic subshowers (from  $\pi^0$  and other short lived particles decay) have energies which are far removed from that of the initial neutrino. Very few hadronic showers induced by neutrino interactions of 100 EeV would display an LPM tail. For the photon to exceed 100 PeV with a probability greater than 2%, the initial neutrino energy should be above 80 EeV.

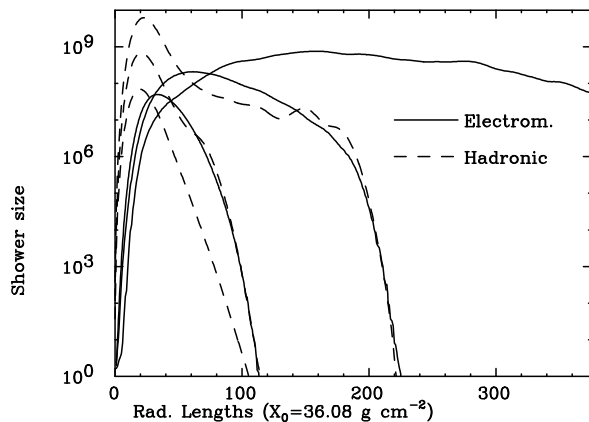


FIG. 3. Longitudinal development of electromagnetic and hadronic showers.

The elongation has a dramatic effect on the angular distribution of the radio pulse. For electromagnetic showers the central peak width narrows as  $E^{-1/3}$  above 20 PeV [16]. A 10 EeV electron produces a pulse which is about 10 times narrower than that of a hadronic shower of the same energy what makes differentiation between pulses from electromagnetic and hadronic cascades possible in principle, allowing the characterization of electron neutrinos (see Fig. 3). For showers initiated by hadrons above 10 EeV the pulse shows a characteristic angular distribution of interference of two periodicities corresponding to the two length scales, one associated to the hadronic shower and the second, longer but of much less intensity associated to the electromagnetic LPM tail [17]. The radio pulse for an electron neutrino interaction

has an interference pattern of similar nature. As the average fraction of energy transfer to the hadron debris is expected to be about  $\langle y \rangle = 0.25$  [23] this interference effect is typically enhanced as shown in Fig. 4. The angular distribution of the pulse retains enough information to allow independent extraction of the total electromagnetic energy in both showers, that is to determine the individual energy transfer of the reaction.

Typical energy thresholds for detecting electromagnetic showers with single antennas have been made in [13,16,17,15] and are typically tens of PeV for showers produced at 1 km from the antenna assuming nominal frequencies of  $\nu_0 = 1$  GHz and bandwidths of  $0.1 \nu_0$ . This corresponds of course to the case that the antenna lies just in the illuminated region of the central peak. The volume of the illuminated region decreases linearly as  $\nu_0$  rises and is also significantly different for electromagnetic and hadronic showers of energy above 100 PeV.

Clearly a signal from a single antenna would be of little use for neutrino detection unless information about the shower direction and/or the shower energy could be obtained from it. If this was not the case it would be impossible to distinguish them from nearby pulses produced by low energy showers such as those induced by deeply penetrating muons. Information on neutrino interactions can only be obtained by placing antennas in an array covering a large region whether on the ice surface or under it [10]. The arrival times for pulses, the polarization [11], the relative amplitudes of the signals, and the frequencies at different positions of the array elements are in principle experimentally accessible and would give relevant and redundant information. The technique is similar to "conventional" neutrino detector proposals but can be highly enriched with the angular diffraction patterns, the frequency spectra and the polarization.

For intermediate energies one looks for events coming from "below" where the Earth provides a shield for all other types of particles. For extremely high energies ( $> 100$  PeV) however the Earth becomes opaque and neutrino events have to be searched in the horizontal direction or possibly from "above". Although some high energy showers can be expected from other processes such as atmospheric muon bremsstrahlung at PeV energies the background of these events is sufficiently suppressed. There is redundant information that allows a variety of cross checks. For instance timing can be used to establish the shower position in a manner very similar to arrays of particle detectors detecting air showers, but the spatial distribution of the signal in the detector can be also used for the same purpose, even signal polarization provides an interesting cross check of the shower orientation, what will also be particularly useful to filter spurious noise signals out.

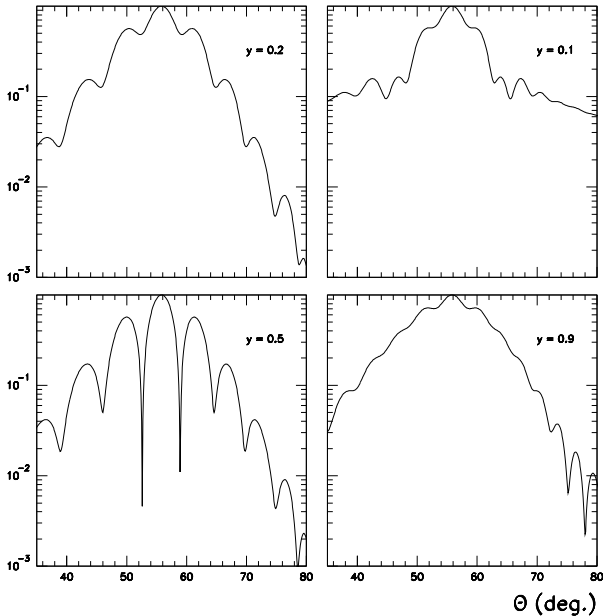


FIG. 4. Interference pattern for  $\nu = 100$  MHz as obtained in charged current neutrino interactions with different energy transfers to the hadron ( $y$ ) as indicated.

The antenna/array parameters are crucial for performance. Most importantly operating frequency  $\nu_0$ , bandwidth  $\Delta\nu$  and array spacing. These parameters are deeply interconnected at detection level and therefore require complex optimization once the noise levels are well understood. The spacing of the antenna array will determine the minimum distance at which the geometry of the illuminated region corresponding to the Cherenkov central peak can be reconstructed, what would indicate the position of the shower [7]. The nominal frequency will determine both the width of the diffraction peaks and the transmitting properties of the medium so that array spacing should be adjusted to the choice of antenna. Lastly the larger the bandwidth the better the signal to noise ratio because the noise behaves as  $\sqrt{\Delta\nu}$ .

Neglecting attenuation the ratio of shower energy to distance has to be above a given value for a shower to be detected. As  $\nu_0$  approaches the naively optimal value for coherence of 1 GHz the attenuation distance drops below 1 km and what is more problematic temperature effects become important [11] possibly forcing detections to be within scales less than 1 km for such antennas. Using lower frequencies the signal to noise ratio drops and higher energy thresholds are needed to compensate the loss of signal. This may be nevertheless advisable if one is ready to concentrate on neutrinos of the highest energies allowing detection at distances above 1 km.

We have discussed the implications of radio pulse calculations for high energy shower detection stressing how different features of the signal can be used for shower characterization. We have shown how the LPM effect allows the separation of charged current electron neu-

trino interactions from the rest, and in principle how the technique can be used to extract the energy fraction transmitted to the electron. We have avoided the discussion of unresolved experimental issues [11,24], i.e. noise, which are likely to determine the final sensitivity of the technique, that is the precise energy value above which showers become detectable over sufficiently long distances. This sensitivity will be also completely dependent on the experimental setup which will have to be optimized accordingly. These crucial issues have to be addressed with in situ experiments and there are efforts in this direction [25], but are unlikely to change the general conclusions obtained here.

**Acknowledgements:** We thank F. Halzen for suggestions after reading the manuscript and G. Parente, T. Stanev and I.M. Zheleznykh for helpful discussions. This work was supported in part by CICYT (AEN96-1773) and by Xunta de Galicia (XUGA-20604A96). J.A. thanks the Xunta de Galicia for financial support.

- 
- [1] T.K. Gaisser, F. Halzen, and T. Stanev, *Phys. Rep.* **258** (1995) 173 and references therein.
  - [2] F. Halzen, *The case for a kilometer-scale neutrino detector*, in *Nuclear and Particle Astrophysics and Cosmology, Proceedings of Snowmass 94*, R. Kolb and R. Peccei, eds.; *The Case for a Kilometer-Scale Neutrino Detector: 1996*, in *Proc. of the Sixth International Symposium on Neutrino Telescopes*, ed. by M. Baldo-Ceolin, Venice (1996).
  - [3] Y. Fukuda *et al.*, *Phys. Rev. Lett.* **81** (1998) 1562.
  - [4] H. Minakata, A. Yu. Smirnov, *Phys. Rev.* **D54** (1996) 3698.
  - [5] K.S. Capelle, J.W. Cronin, G. Parente, and E. Zas, *Astro. Phys.* **8** (1998) 321.
  - [6] G.A. Askar'yan, *Soviet Physics JETP* **14** (1962)2 441; **48** (1965) 988.
  - [7] M.A. Markov and I.M. Zheleznykh, *Nucl. Instr. and Methods in Phys. Research* **A248** (1986) 242.
  - [8] P.B. Price, *Astro. Phys.* **5** (1996) 43.
  - [9] I. Frank, I. Tamm, *Dokl. Akad. Nauk SSSR* **14** 109 (1937).
  - [10] G.M. Frichter *et al.*, *Phys. Rev.* **D53**,3 (1996), 1684.
  - [11] H.R. Allan, *Progress in Elementary Particles and Cosmic Ray Physics* (North Holland, 1971), Vol. 10, p. 171.
  - [12] J.V. Jelley, *Astro. Phys.* **5** (1996) 255 and refs. therein.
  - [13] E. Zas, F. Halzen, T. Stanev, *Phys. Rev.* **D45** (1992) 362.
  - [14] F. Halzen, E. Zas, T. Stanev, *Phys. Lett.* **B257** 1991 432.
  - [15] A.L. Provorov, I.M. Zheleznykh, *Astro. Phys.* **4** (1995) 55.
  - [16] J. Alvarez-Muñiz, E. Zas, *Phys. Lett.* **B411** 218 1997.
  - [17] J. Alvarez-Muñiz, E. Zas, *Phys. Lett.* **B434** 396 (1998).
  - [18] J. Alvarez-Muñiz and E. Zas, work in preparation.

- [19] K. Greisen, Prog. of Cosmic Ray Phys., ed. J.G. Wilson, Vol. III, (North Holland, 1956) p.1.
- [20] T. Stanev et al. Phys. Rev. **D25** (1982) 1291.
- [21] L. Landau and I. Pomeranchuk, *Dokl. Akad. Nauk SSSR* **92** (1953) 535; **92** (1935) 735; A.B. Migdal, Phys. Rev. **103** (1956) 1811; Sov. Phys. JETP **5** (1957) 527.
- [22] S.R. Klein, hep-ph/9802442, to be publ. in Rev. Mod. Phys; also astro-ph/9712198.
- [23] J. Castro, G. Parente, and E. Zas, in preparation.
- [24] I.M. Zheleznykh, *Proc. XXIth ICRC* (Adelaide, 1989), Vol. 6, p. 528.
- [25] C. Allen *et al.* *Proc. High Energy Physics Conf.* 1998.